SCIENTIFIC CULTURE

SCIENTIFIC CULTURE, Vol. 3, No. 2, (2017), pp. 7-12
Open Access. Online & Print

DOI: 10.5281/zenodo.438182

A COMPARATIVE STUDY OF THE WETTING PROPERTIES OF A SUPERHYDROPHOBIC SILOXANE MATERIAL AND ROSE PETAL

Panagiotis N. Manoudis, Dafni Gemenetzis and Ioannis Karapanagiotis*

Department of Management and Conservation of Ecclesiastical Cultural Heritage Objects, University Ecclesiastical Academy of Thessaloniki, Thessaloniki 54250, Greece

Received: 06/12/2016
Accepted: 20/03/2017
Corresponding author: y.karapanagiotis@aeath.gr

ABSTRACT

Polysiloxane materials have been used in conservation and protection of stone monuments and other outdoor objects of the cultural heritage for decades. Enhancing the inherent hydrophobic character of the siloxane materials is highly desirable as it can promote their protection efficacy against the degradation effects which are induced by rain water and/or humidity. We show that mixing a solution of a polysiloxane material with a small amount (1% w/w) of silica nanoparticles leads to the formation of a structured surface which has superhydrophobic properties i.e. the contact angle (CA) of a water droplet on the surface of the polysiloxane+nanoparticle film is >150°.

We monitor the evaporation process of the water droplet on the surface of the composite (polysiloxane+nanoparticle) film and show that it follows the same evaporation mode reported for a water droplet resting on the surface of a natural rose petal. In particular, the evaporation of droplets on both composite and natural surfaces follows the constant contact radius (CCR) mode: the contact area between water and surface remains constant with time and the contact angle decreases. Moreover, we report that in the course of evaporation the relationship of the volume of the droplet to the 2/3 power ($V^{2/3}$) with time (t) is linear.

KEYWORDS: siloxane, rose, nanoparticle, superhydrophobic, evaporation, drop, stone, conservation.

1. INTRODUCTION

Water that originates from humidity or rain can cause decay of stone monuments by freezing-thawing cycles, crystallization of salts, and chemical reactions initiated by atmospheric pollutants that are carried by water. For this reason, the application of hydrophobic coatings has been suggested in the past for the surface protection of outdoor cultural heritage assets (Allesandrini et al., 2000; Borgia et al., 2003; Chiantore and Lazzari, 2001; Toniolo et al., 2002; Tsakalof et al., 2007). Hydrophobicity and other wetting regimes are defined by the contact angle of a water droplet resting on a solid, passive surface, as shown in Figure 1. In the last two decades, several strategies have been devised to produce superhydrophobic surfaces, which, in principle, can offer better protection to the outdoor objects against water induced effects, as discussed in several review articles e.g. (Mohamed et al., 2015; Zhang et al., 2016; Zhang and Lv, 2015). As these strategies consist in mimicking the hierarchical structured biosurfaces, found in plants and animals, superhydrophobic surfaces are considered as biomimetics materials.

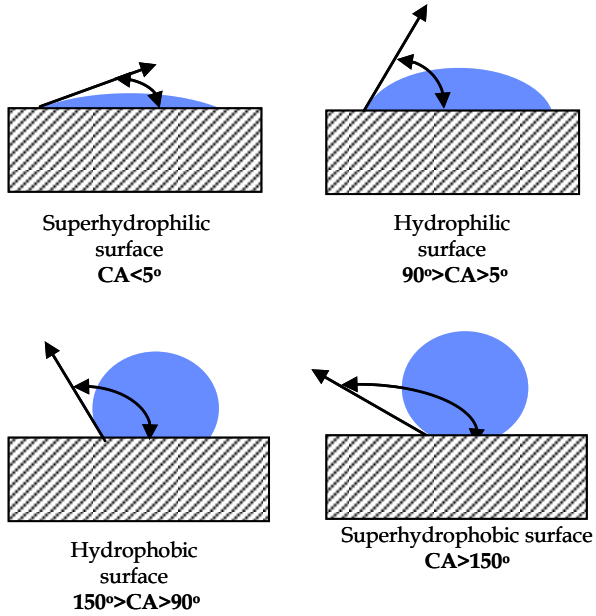

Figure 1. The four wetting regimes as defined by the contact angle (CA) between a water droplet and a surface.

The surfaces of the lotus leaf and rose petal have been extensively used as model surfaces to fabricate biomimetics materials of special and controlled wettabilities (Barthlott and Neinhuis, 1997; Feng et al., 2008). Both biological surfaces exhibit superhydrophobic properties, implying that the static contact angle (CA) of a resting water droplet is large, CA>150° (Figure 1). However, the two plant surfaces show different dynamic wetting. That is, water droplets can effortlessly roll off the surface of a lotus leaf ("lotus effect") whereas they stay pinned to the surface of a red rose petal ("petal effect") (Barthlott and Neinhuis, 1997; Feng et al., 2008).

The evaporation of water droplets on a surface is extremely important to understand the behaviour of the surface wettability. In 1977 Picknett and Bexon identified two extreme modes in the evaporation of droplets on surfaces (Picknett and Bexon, 1977): the constant contact angle mode, usually abbreviated to CCA, where CA is unaltered during evaporation, the droplet shape remaining that of a spherical cap but with diminishing area of contact between liquid and surface. In the second, called the constant contact area or radius mode, hereafter CCR, evaporation takes place with unchanged contact area between liquid and surface, the shape remaining that of a spherical cap but with diminishing CA (Picknett and Bexon, 1977). Furthermore, Picknett and Bexon showed that a mixed mode, where both contact angle and contact radius decrease together, does also exist.

Based on the early work of Picknett and Bexon, the evaporation of water droplets on various superhydrophobic surfaces, has been recently investigated (Chen et al., 2012; Dash and Garimella, 2013; Dash et al., 2011; Gelderblom et al., 2011; Gjerde et al., 2008; Karapanagiotis et al., 2016; Karapanagiotis et al., 2014; Kulinich and Farzaneh, 2009a; Kulinich and Farzaneh, 2009b; McHale et al., 2005; Song et al., 2005; Teisala et al., 2012; Xu et al., 2013; Yu et al., 2013; Zhang et al., 2006). We monitor the evaporation process of water drops on a superhycrophobic poly(alkyl siloxane) surface which was roughened by adding silica nanoparticles. Polysiloxanes are extensively used for the protection and consolidation of stone monuments (Wheeler, 2005). Adding nanoparticles into a polymer matrix to induce superhydrophobicity, thus achieving large contact angles (CA>150°) with water drops, is an easy, low cost processing route, which has therefore become a standard method. We show that water drops on the fabricated polysiloxane+nanoparticle composite film are pinned, implying similar wettability with that of the rose petal surface. For this reason, we first monitor the evaporation process of a water droplet on the natural surface of the rose petal. The results provide the basis to gain a better understanding on the wetting properties of the composite film.

2. EXPERIMENTAL

Silres BS290, which is a poly(alkyl siloxane) provided by Wacker, was dissolved in white spirit to prepare a solution of 7% w/w. Silica (SiO_2) nanoparticles (Aldrich) with a 7 nm mean diameter were added in the solution to prepare a dispersion of 1% w/w which was spin coated onto clean glass slides

(Wheel Brand). The film was annealed at 40°C overnight to remove residual solvent. Fresh roses, obtained from the local market, were cleaned with distilled water and dried.

The evaporation of water droplets resting on the surfaces of the rose petal and the polysiloxane+nanoparticle film was monitored at room conditions using an optical tensiometer (Attension Theta) which was set to capture successive snapshots of the droplet. Scanning electron microscopy (SEM; JEOL, JSM-6510) was employed to study the structures of the surfaces.

3. RESULTS AND DISCUSSION

Figure 2 shows a SEM image of the surface of the rose petal. A periodic array of micropapillae is revealed, with an average diameter ranging within 10-20μm. Clearly, the protruded micropapillae are not smooth, as they do exhibit structures at the nanometer scale. Therefore, a two-length scale hierarchical structure is revealed on the surface of the rose petal, as shown in Figure 2 and described in previously published reports (Feng et al., 2008). The special surface structure induces superhydrophobic properties to the rose petal surface, implying that the static contact angle (CA) of a resting water droplet is large, CA>150°, so that the shape of the droplet tends to that of a sphere (Figure 2). In our study, the CA measured immediately after droplet deposition was 153° which is in excellent agreement with previously reported measurements on rose petal surfaces (Feng et al., 2008). In the case of the rose petal, the observed superhydrophobicity is not accompanied by water repellency. The droplet is pinned and cannot roll off even when the petal is tilted vertically, by 90°, as shown in the photograph of Figure 2, thus implying high droplet adhesion (Feng et al., 2008).

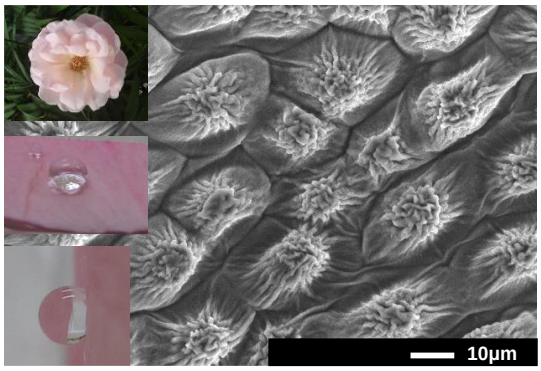

Figure 2. SEM image of the surface of the rose petal, revealing a periodic array of micropapillae which consist of nanostructures. Photographs shown water droplets on horizontal and vertically tilted (by 90°) rose petal surfaces are included.

Figure 3 shows the dependence of CA and radius (R) of the droplet-petal contact against time, t, in the course of evaporation. R remains constant during the experiment. On the other hand, CA decreases with t. The results of Figure 3 clearly suggest that the droplet evaporation on the surface of the rose petal is dominated by the CCR mode. This result is in agreement with a previously published report (Teisala et al., 2011): evaporation takes place with unchanged R and diminishing CA. The pinned three-phase contact line observed during water evaporation on the rose petal indicates high droplet adhesion so that the dynamic free energy cannot overcome the energy barrier for the three phase line transition (Zhang et al., 2006). Consequently, the CCR mode of evaporation revealed in Figure 3, is in agreement with the scenario of the pinned droplet on a vertically tilted rose petal, shown in Figure 2.

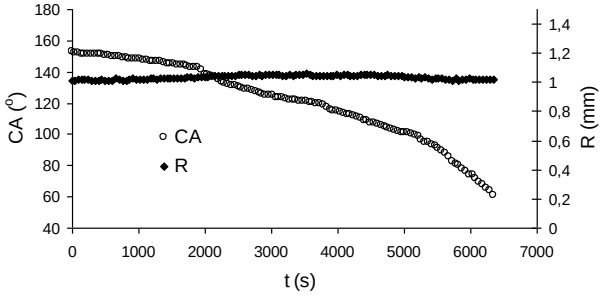

Figure 3. Contact angle (CA) and contact radius (R) of a droplet on the surface of the rose petal versus evaporation time (t). The CCR mode of evaporation is recorded. The scale of the contact diameter 2R is smaller than the capillary length, κ^{-1}, which is $\kappa^{-1}=(\gamma/\rho g)^{1/2}$ where γ and ρ are the surface tension and density of water, respectively, and g is the acceleration due to gravity. For water at room temperature, κ^{-1}=2.7 mm. Consequently, gravitational effects on the CA measurements reported in the graph can be considered as negligible.

The variation of the volume (V) of the droplet to the 2/3 power with t is shown in Figure 4. The volume is normalized to its initial (Vo) value. It is seen that a linear relationship between $(V/Vo)^{2/3}$ and t is a very good fitting. The results of Figure 4 offer support to previously published reports (Karapanagiotis et al., 2014; Xu et al., 2013) which suggested that the power-law relationship ($V^{2/3}$~t) predicts the evaporation process on a superhydrophobic surface more accurately than the linear model (V~t) suggested for the CCR evaporation of a droplet on a hydrophilic surface (Birdi et al., 1989; Hu and Larson, 2002). The rate of evaporation of the droplet is expressed as follows:

$$\text{rate} = -\frac{dm}{dt} = -\rho\frac{dV}{dt} \quad (1)$$

where m and V are the mass and the volume of the droplet, respectively, and ρ the density of the liquid. The power-law relationship ($V^{2/3}$~t) used in Figure 4 implies that evaporation is slower on the rose petal surface than on a hydrophilic surface, where V~t.

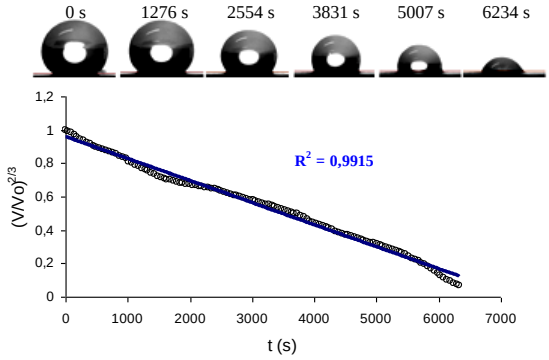

Figure 4. Normalized droplet volume to the 2/3 power versus evaporation time t for a droplet on the surface of the rose petal. A linear relationship is used to fit the data, resulting in a coefficient of determination (R^2) close to one. Successive snapshots of a droplet captured during evaporation are shown.

We now turn our attention on the wetting properties of the polysiloxane+nanoparticle film. The surface of the film is revealed by the SEM image of Figure 5. The use of nanoparticles results in the formation of microscale clusters with nanostructures. The clusters are separated by areas of no special structure. A surface roughness at the micrometer and nanometer scale is formed corresponding to a two-length scale hierarchical structure, as noticed also for the surface of the rose petal (Figure 2). The structure revealed in Figure 5 is in perfect agreement with previously published studies which described the effect of nanoparticles on the surface of polymer+nanoparticle composite films (Manoudis et al., 2008; Tiwari et al., 2010).

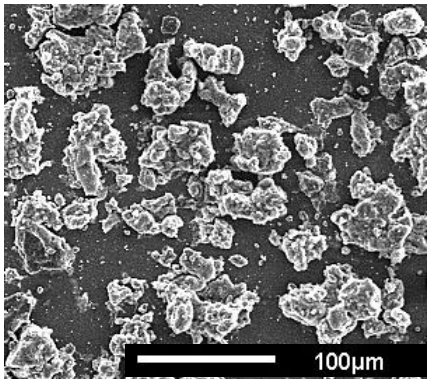

Figure 5. SEM image of the surface of a polysiloxane+nanopaticle (Silres BS290+SiO_2) film, revealing microscale clusters consisted of nanostructures.

Figure 6 shows the evolution of CA and R of a water drop on the polysiloxane+nanoparticle film. The CA measured immediately after droplet deposition (t=0) was 155° thus showing that superhydrophobicity was achieved. This high CA indicates that the hydrophilic SiO_2 nanoparticles contribute only to the creation of the roughness of the surface which is covered by the hydrophobic siloxane material, as suggested in previously published reports (Karapanagiotis et al. 2016; Kulinich and Farzaneh, 2009a; Kulinich and Farzaneh, 2009b). Overall, the results in Figure 6 follow the same trend captured in Figure 3 for the surface of the rose petal. A water droplet on the polysiloxane+nanoparticle film evaporates with unchanged R and diminishing CA. The CCR mode dominates the evaporation process in Figure 6, implying that the drop is pinned on the surface. Indeed, water drops on the produced polysiloxane+nanoparticle film remained pinned on the surface even when these were tilted by very high angles. Pinned drops on siloxane surfaces were reported by Song and co-workers (Song et al., 2005) who argued that the strong interaction between the hydrophilic silanol groups and water are responsible for the observed interaction.

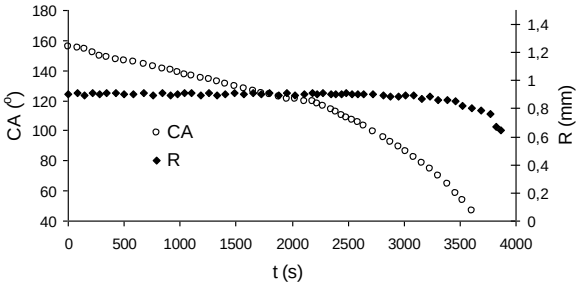

Figure 6. Contact angle (CA) and contact radius (R) of a droplet on the surface of the polysiloxane+nanoparticle film versus evaporation time (t). The CCR mode of evaporation is recorded. The scale of the contact diameter 2R is smaller than the capillary length, κ^{-1} (=2.7 mm).

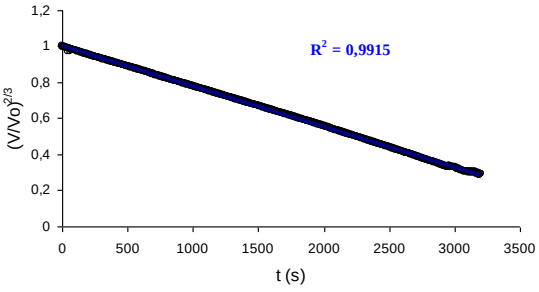

Figure 7. Normalized droplet volume to the 2/3 power versus evaporation time t for a droplet on the surface of the polysiloxane+nanoparticle film. A linear relationship is used to fit the data, resulting in a coefficient of determination (R^2) close to one.

Finally, Figure 7 shows that a linear relationship between the volume of the droplet to the 2/3 power

with time was recorded in the course of evaporation of the water droplet on the polysiloxane+nanoparticle film, similar to what it was observed for the rose petal (Figure 4). Consequently, the fabricated polysiloxane+nanoparticle film shows qualitatively the same wetting properties with the surface of the rose petal.

4. CONCLUSIONS

Superhydrophobicity was induced in a poly(alkyl siloxane) material by embedding a small amount of silica nanoparticles (7nm in mean diameter). The contact angle (CA) of a water droplet on the surface of the polysiloxane+nanoparticle composite film was 155° which is close to the CA=153° measured for droplets resting on the surface of the rose petal.

On the surfaces of both composite film and rose petal, water droplets evaporate according to the constant contact radius (CCR) mode: the contact radius between the droplet and the surface remains constant with time whereas the contact angle decreases from 155° and 153° to small values. Finally, it was shown that in the course of evaporation the relationship of the volume of the droplet to the 2/3 power with time is linear.

REFERENCES

Allesandrini, G., Aglietto, M., Castelvetro, V., Ciardelli, F., Peruzzi, R., Toniolo, L. (2000) Comparative evaluation of fluorinated and unfluorinated acrylic copolymers as water-repellent coating materials for stone. *J. Appl. Polym. Sci.*, Vol. 76, 962–977.

Barthlott, W., Neinhuis, C. (1997) Purity of the sacred lotus, or escape from contamination in biological surfaces. *Planta*, Vol. 202, 1–8.

Birdi, K.S., Vu, D.T., Winter, A. (1989) A study of the evaporation rates of small water drops placed on a solid surface. *J. Phys. Chem.*, Vol. 93, 3702–3703.

Borgia, G.C., Piace, F., Camaiti, M., Cerri, F., Fantazzini, P., Piacenti F. (2003) Hydrophobic treatments for stone conservation: influence of the application method on penetration, distribution, and efficiency. *Stud. Conserv.*, Vol. 48, 217–226.

Chen, X., Ma, R., Li, J., Hao, C., Guo, W., Luk, B. L., Li, S. C., Yao, S., Wang, Z. (2012) Evaporation of droplets on superhydrophobic surfaces: surface roughness and small droplet size effects. *Phys. Rev. Lett.*, Vol. 109, 116101.

Chiantore, O., Lazzari, M. (2001) Photo-oxidative stability of Paraloid acrylic protective polymers. *Polymer*, Vol. 42, 17–27.

Dash, S., Garimella, S.V. (2013) Droplet evaporation dynamics on a superhydrophobic surface with negligible hysteresis. *Langmuir*, Vol. 29, 10785–10795.

Dash, S., Kumari, N., Garimella, S.V. (2011) Characterization of ultrahydrophobic hierarchical surfaces fabricated using single-step fabrication methodology. *J. Micromech. Microeng.*, Vol. 21, 105012.

Feng, L., Zhang, Y., Xi, J., Zhu, Y., Wang, N., Xia, F., Jiang, L. (2008) Petal effect: a superhydrophobic state with high adhesive force. *Langmuir*, Vol. 24, 4114–4119.

Gelderblom, H., Marín, Á.G., Nair, H., van Houselt, A., Lefferts, L., Snoeijer, J.H., Lohse, D. (2011) How water droplets evaporate on a superhydrophobic substrate. *Phys. Rev. E*, Vol. 83, 026306.

Gjerde, K., Rajendra-Kumar, R.T., Nordstrom-Andersen, K., Kjelstrup-Hansen, J., Teo, K.B.K., Milne, W.I., Persson, C., Molhave, K., Ruabahn, H.-G., Boggild, P. (2008) On the suitability of carbon nanotube forests as non-stick surfaces for nanomanipulation. *Soft Matter*, Vol. 4, 392–399.

Hu, H., Larson, R.G. (2002) Evaporation of a sessile droplet on a substrate. *J. Phys. Chem. B*, Vol. 106, 1334–1344.

Karapanagiotis, I., Manoudis, P.N., Zurba, A., Lampakis, D. (2014) From hydrophobic to superhydrophobic and superhydrophilic siloxanes by thermal treatment. *Langmuir*, Vol. 30, 13235–13243.

Karapanagiotis, I., Aifantis K.E., Konstantinidis A. (2016) Capturing the evaporation process of water drops on sticky superhydrophobic polymer-nanoparticle surfaces, *Materials Letters*, Vol. 164, 117–119.

Kulinich, SA., Farzaneh, M. (2009a) Effect of contact angle hysteresis on water droplet evaporation from super-hydrophobic surfaces. *Appl. Surf. Sci.*, Vol. 255, 4056–4060.

Kulinich, S.A., Farzaneh, M. (2009b) How wetting hysteresis influences ice adhesion strength on superhydrophobic surfaces. *Langmuir*, Vol. 25, 8854–8856.

Manoudis, P.N., Karapanagiotis, I., Tsakalof, A., Zubirtikudis, I., Panayiotou C. (2008) Superhydrophobic composite films produced on various substrates. *Langmuir*, Vol. 24, 11225–11232.

McHale, G., Aqil, S., Shirtcliffe, N.J., Newton, M.I., Erbil, H.Y. (2005) Analysis of droplet evaporation on a superhydrophobic surface. *Langmuir*, Vol. 21, 11053–11060.

Mohamed, A.M.A., Abdullah, A.M., Younan, N.A. (2015) Corrosion behavior of superhydrophobic surfaces: A review. *Arab. J. Chem.*, Vol. 8, 749–765.

Picknett, R.G., Bexon, R.J. (1977) The evaporation of sessile or pendant drops in still air. *J. Colloid Interface Sci.*, Vol. 61, 336–350.

Song, X., Zhai, J., Wang, Y., Jiang, L. (2005) Fabrication of superhydrophobic surfaces by self-assembly and their water-adhesion properties. *J. Phys. Chem. B*, Vol. 109, 4048–4052.

Teisala, H., Tuominen, M., Aromaa, M., Stepien, M., Ma ̈kela ̈, J.M., Saarinen, J.J., Toivakka, M., Kuusipalo, J. (2012) Nanostructures increase water droplet adhesion on hierarchically rough superhydrophobic surfaces. *Langmuir*, Vol. 28, 3138–3145.

Teisala, H., Tuominen, M., Kuusipalo J. (2011) Adhesion mechanism of water droplets on hierarchically rough superhydrophobic rose petal surface. *Journal of Nanomaterials*, Article ID 818707.

Tiwari, M.K., Bayer, I.S., Jursich, G.M., Schutzius, T.M., Megaridis, C.M. (2010) Highly liquid-repellent, large-area, nanostructured poly(vinylidenefluoride)/poly(ethyl2-cyanoacrylate) composite coatings: particle filler effects. *ACS Appl. Mater. Inter. Vol.*, 2, 1114–1119.

Toniolo, L., Poli, T., Castelvetro, V., Manariti, A., Chiantore, O., Lazzari, M. (2002) Tailoring new fluorinated acrylic copolymers as protective coatings for marble. *J. Cult. Herit.*, Vol. 3, 309–316.

Tsakalof, A., Manoudis, P., Karapanagiotis, I., Chryssoulakis, I., Panayiotou, C. (2007) Assessment of synthetic polymeric coatings for the protection and preservation of stone monuments, *J. Cult. Herit.*, Vol. 8, 69 – 72.

Wheeler (2005) *Alkoxysilanes and the consolidation of stone*, Getty Publications, LA, USA.

Xu, W., Leeladhar, R., Kang, Y.T., Choi, C-H. (2013) Evaporation kinetics of sessile water droplets on micropillared superhydrophobic surfaces. *Langmuir*, Vol. 29, 6032–60341.

Yu, Y. -S., Wang, Z. -Q., Zhao, Y. -P. (2013) Experimental study of evaporation of sessile water droplet on PDMS surfaces. *Acta Mech. Sinica*, Vol. 29, 799–805.

Zhang, M., Feng, S., Wang, L., Zheng, Y. (2016) Lotus effect in wetting and self-cleaning. *Biotribology*, Vol. 5, 31–43.

Zhang, P., Lv, F.Y. (2015) A review of the recent advances in superhydrophobic surfaces and the emerging energy-related applications. *Energy*, Vol. 82, 1068–1087.

Zhang, X., Tan, S., Zhao, N., Guo, X., Zhang, X., Zhang, Y., Xu, J. (2006) Evaporation of sessile water droplets on superhydrophobic natural lotus and biomimetic polymer surfaces. *Chem. Phys. Chem.*, Vol. 7, 2067–2070.